

Review paper

# Mechanical behavior and ultrasonic non-destructive characterization of elastic properties of cordierite-based ceramics

A. Benhammou<sup>a,b,\*</sup>, Y. El Hafiane<sup>a</sup>, L. Nibou<sup>a</sup>, A. Yaacoubi<sup>b</sup>, J. Soro<sup>c</sup>, A. Smith<sup>c</sup>,  
J.P. Bonnet<sup>c</sup>, B. Tanouti<sup>b</sup>

<sup>a</sup>Laboratoire Matériaux, Procédés, Environnement et Qualité, Ecole Nationale des Sciences Appliquées, Route Sidi Bouzid, BP 63, Safi, Morocco

<sup>b</sup>Laboratoire de la Matière Condensée et de l'Environnement, Faculté des Sciences Semlalia, Avenue My Abdellah, BP 2390, Marrakech, Morocco

<sup>c</sup>Groupe d'Etude des Matériaux Hétérogènes, ENSCI, 47-73, Avenue Albert Thomas, 11 87065 Limoges Cedex, France

Received 4 March 2011; received in revised form 15 June 2012; accepted 20 June 2012

Available online 28 June 2012

## Abstract

The structural and morphological evolutions of cordierite-based ceramics produced from stevensite/andalusite mixture sintered from 1150 to 1350 °C were studied using X-ray diffraction (XRD) and scanning electron microscopy (SEM). The mechanical behavior was investigated by three-point bending and Brazilian tests. The elastic properties were evaluated using ultrasonic non-destructive testing (NDT). XRD results revealed that the main crystalline phase formed at 1300 and 1350 °C was cordierite with traces of mullite. A linear-elastic behavior followed by brittle fracture was observed in three-point bending test with the presence of multiple discontinuities. Flexural and diametral compression strength values of cordierite sintered at 1300 °C were  $39.4 \pm 4$  and  $21.8 \pm 2$  MPa, respectively. The elastic properties such as Young's modulus (38.7–45.1 GPa), shear modulus (17.90–19.42 GPa) and Poisson ratio (0.08–1.6) of cordierite-based ceramics produced at 1350 and 1300 °C were also determined.

© 2012 Elsevier Ltd and Techna Group S.r.l. All rights reserved.

**Keywords:** D. Cordierite; Elastic properties; Mechanical behavior; Ultrasonic testing

## Contents

1. Introduction	22
2. Materials and methods	22
2.1. Materials	22
2.2. Characterization techniques	22
2.3. Three-point bending test	22
2.4. Brazilian test	23
2.5. Elastic properties	23
3. Results and discussion	23
3.1. Phase evolution during sintering	23
3.2. Densification evolution during sintering	24
3.3. Mechanical properties	24
3.3.1. Three-point bending test	24

\*Corresponding author at: Laboratoire Matériaux, Procédés, Environnement et Qualité, Ecole Nationale des Sciences Appliquées, Route Sidi Bouzid, BP 63, Safi, Morocco. Tel.: +212 024 66 91 55; fax: +212 024 66 80 12.

E-mail address: [Benhammou\\_ab@yahoo.fr](mailto:Benhammou_ab@yahoo.fr) (A. Benhammou).

3.3.2.	Brazilian test . . . . .	25
3.3.3.	Elastic properties . . . . .	26
4.	Conclusion . . . . .	26
	References . . . . .	26

## 1. Introduction

Cordierite-based ceramics ( $2\text{MgO} \cdot 2\text{Al}_2\text{O}_3 \cdot 5\text{SiO}_2$ ) due to its good mechanical and thermal properties are considered as potential candidate for advanced applications in varied fields. These materials are extensively used as refractory products, filtration, electroceramics and catalyst carriers [1–4]. Many authors have reported the preparation of cordierite by various techniques and from various raw materials in order to optimize the fabrication process and to obtain the enhanced properties [5–7]. The preparation of cordierite ceramics by solid-state reaction technique from stoichiometric mixtures of clays (kaolinite, vermiculite, sepiolite, feldspar), talc and diatomite has been studied [8–10]. Kumar et al. [11] reported that fly ash could be used as a substitute material for clay in the synthesis of cordierite for refractory applications. The sol–gel process has been widely studied in recent years to synthesize cordierite at low sintering temperature [12,13].

The synthesis of dense or porous cordierite ceramics was investigated by several authors using various techniques. The presence of porosity in a material is often viewed as inconvenient. However, there are many applications in which the use of porous materials can be necessary, for example in filters, membranes, catalytic substrates, gas burner media, and as refractory materials. A porous cordierite was developed for its feasibility as a filter [14]. The enhancement of mechanical properties by synthesis of dense cordierite by adding various amounts of mullite or  $\text{ZrO}_2$  was studied [15,16]. Generally, the mechanical properties of materials are improved by increasing the sintering temperature so long as it is lower than the maximum shrinkage temperature. Above this temperature a decrease of the mechanical properties is observed and associated to swelling.

This paper presents experimental results on the synthesis and characterization of mechanical properties of cordierite-based ceramics produced from stevensite and andalusite mixture. The structural and morphological evolution of samples sintered between 1150 and 1350 °C were examined by X-ray diffraction (XRD) and scanning electron microscopy (SEM), respectively. Densities and open porosity values were measured by Archimedes method. Three-point bending test, Brazilian test and ultrasonic non-destructive testing (NDT) were used to evaluate the mechanical properties.

## 2. Materials and methods

### 2.1. Materials

The Moroccan raw materials used in this study for cordierite synthesis are andalusite from Sidi Bouatmane

and Ghassoul clay which is composed mainly of stevensite. The Ghassoul clay commercialized by the Moroccan company “Société du Ghassoul et de ses dérivés Sefrioui” is used mostly in cosmetic applications. The chemical composition of stevensite is 57.49%  $\text{SiO}_2$ , 2.24%  $\text{Al}_2\text{O}_3$ , 1.35%  $\text{Fe}_2\text{O}_3$ , 1.46%  $\text{CaO}$ , 25.03%  $\text{MgO}$ , 0.73%  $\text{K}_2\text{O}$  and 0.51%  $\text{Na}_2\text{O}$  [17]. The chemical composition of andalusite from Sidi Bouatmane is 38.50%  $\text{SiO}_2$ , 57.06%  $\text{Al}_2\text{O}_3$ , 1.37%  $\text{Fe}_2\text{O}_3$ , 0.10%  $\text{CaO}$ , 0.13%  $\text{MgO}$ , 0.20%  $\text{K}_2\text{O}$  and 0.05%  $\text{Na}_2\text{O}$  [18]. The mixture prepared in the stoichiometric ratio close to cordierite ( $2\text{MgO} \cdot 2\text{Al}_2\text{O}_3 \cdot 5\text{SiO}_2$ ) is 43.7% of stevensite and 56.3% of andalusite. These raw materials were first crushed to a size lower than 40  $\mu\text{m}$ , homogenized, uniaxially dry pressed under 6 MPa and then sintered at temperature in the range 1150–1350 °C for 2 h with a heating rate of 10 °C  $\text{min}^{-1}$ .

### 2.2. Characterization techniques

The study of phase changes during sintering was performed by X-ray diffraction (XRD) (Siemens D500 instrument, equipped with a monochromator,  $\text{Cu K}\alpha$  radiation). Microstructural characterizations of the sintered samples were carried out using a scanning electron microscope (SEM Stereoscan S260). The density and open porosity of samples sintered between 1150 and 1350 °C were measured by Archimedes principle.

### 2.3. Three-point bending test

The three-point bending test was performed at room temperature using a universal testing machine (Ametek Lloyd Instruments). The test was run at a displacement rate of 0.1 mm  $\text{min}^{-1}$  until specimen failure. Thickness, width and length of specimens were 6, 9 and 60 mm, respectively. The flexural strength and Young's modulus were calculated from linear elasticity theory as follows:

$$\sigma_f = \frac{3}{2} \frac{F L}{w t^2} \quad (1)$$

$$E_s = \frac{F L^3}{48 I f} \quad (2)$$

where  $F$  is the load at fracture,  $w$  and  $t$  are respectively the width and the thickness of the specimen,  $L$  is the distance between supports (50 mm),  $f$  is the loading point displacement (mm), and  $I$  is the moment of inertia  $I = w t^3 / 12$

## 2.4. Brazilian test

The Brazilian test was performed at ambient temperature on cylindrical samples with a diameter of 22 mm and a height of 3 mm. The indirect tensile strength was calculated by the following formula:

$$\sigma_T = \frac{F}{S} = \frac{2F}{\pi D h} \quad (3)$$

where  $F$  is the applied load,  $D$  is the sample diameter and  $h$  is the height.

## 2.5. Elastic properties

The properties of elasticity were determined by ultrasonic echography as a non-destructive testing (NDT) using a Panametric Sofranel instrument. The tests were carried out on cylindrical specimens with a diameter of 32 mm and a thickness of 3 mm. Pulse-echo measurements of ultrasonic waves velocity were used to determine the elastic properties of the cordierite synthesized at 1300 and 1350 °C. The velocity of sound was calculated from the equation:

$$V = \frac{2t}{\tau} \quad (4)$$

where  $V$ ,  $t$ , and  $\tau$  are the velocity of sound, the thickness of the sample, and the time delay between two successive echoes, respectively.

The elastic properties such as the dynamic Young's modulus ( $E_D$ ), shear modulus ( $G$ ) and Poisson's ratio ( $\nu$ ) were evaluated according to the following formulas:

$$E_D = \rho \frac{(3V_L^2 - 4V_T^2)}{\left(\frac{V_L^2}{V_T^2} - 1\right)} \quad (5)$$

$$G = \rho V_T^2 \quad (6)$$

$$\nu = \frac{E_D}{2G} - 1 \quad (7)$$

where  $V_L$ ,  $V_T$  and  $\rho$  are the longitudinal and transverse wave velocity ( $\text{m s}^{-1}$ ) and density of the sample ( $\text{g cm}^{-3}$ ), respectively.

## 3. Results and discussion

### 3.1. Phase evolution during sintering

The XRD patterns of the andalusite/stevensite mixture after dry pressing and sintering for 2 h at 1150, 1200, 1250, 1300 and 1350 °C are shown in Fig. 1. From 1150 to 1250 °C, the main phase observed was andalusite with a significant amount of cordierite. Small amounts of cristobalite ( $\text{SiO}_2$ ), enstatite ( $\text{MgOSiO}_2$ ) and spinel ( $\text{MgOAl}_2\text{O}_3$ ) phases were also detected. The appearance of enstatite and cristobalite phases may be attributed to the thermal

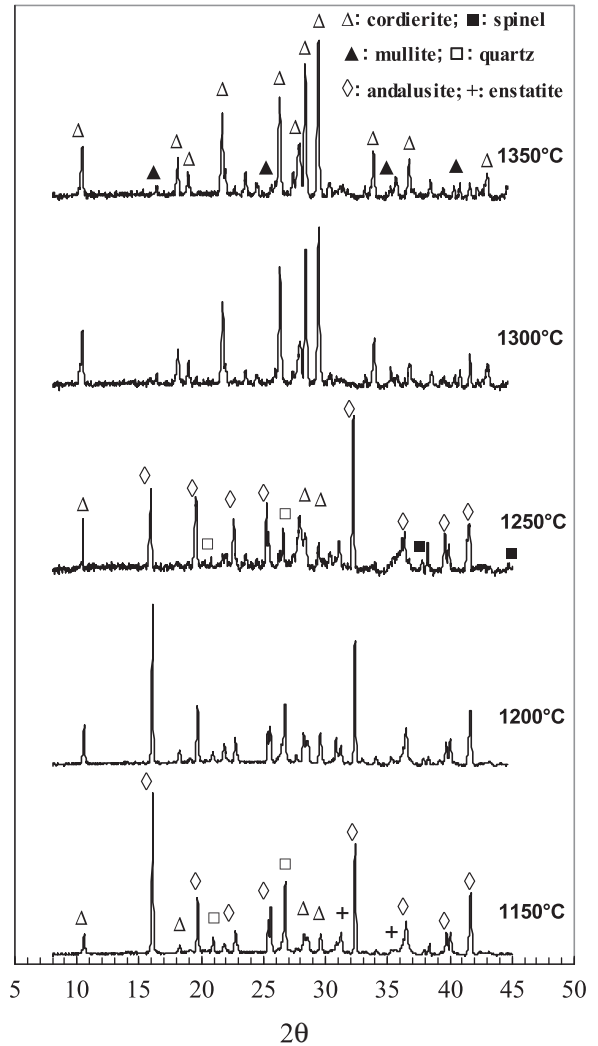
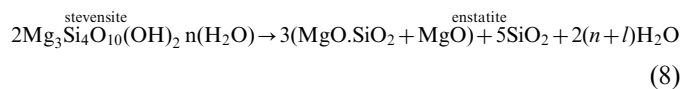
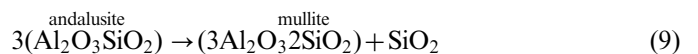


Fig. 1. XRD patterns of samples fired at different temperatures.

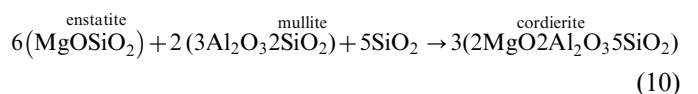
decomposition of stevensite as follows [19]



At 1300 °C and 1350 °C, the main crystalline phase formed was cordierite with traces of mullite ( $3\text{Al}_2\text{O}_3 \cdot 2\text{SiO}_2$ ). Previous studies have shown that the mullite and silica formation is due to the thermal decomposition of andalusite ( $\text{Al}_2\text{O}_3 \cdot \text{SiO}_2$ ) according to the reaction [20]:



The reflection intensities of enstatite, spinel, cristobalite and andalusite were disappeared, indicating that these phases were consumed in favor of the cordierite formation. The cordierite formation may be attributed to the reaction between enstatite, mullite and silica liquid:



The cordierite can also be produced from the reaction between spinel and silica liquid as follow:



### 3.2. Densification evolution during sintering

Fig. 2 shows the relative density and open porosity evolution of the andalusite-stevensite mixture sintered at different temperatures between 1150 and 1350 °C. A small increase in relative density from 73 to 78% was initially observed when the sintering temperature was increased from 1150 to 1250 °C. This is probably due to the increase in the amount of liquid phase with increasing temperature and consequently, the densification of the material. The vitreous phase formation may be attributed to the thermal decomposition of andalusite ( $\text{Al}_2\text{O}_3\text{SiO}_2$ ) into mullite ( $3\text{Al}_2\text{O}_3\text{SiO}_2$ ) and silica phase ( $\text{SiO}_2$ ), mainly in a vitreous form [20]. The liquid phase formation can also be explained by the presence of impurities in raw materials, namely the fluxing elements such as (K, Na, Ca, Mg, etc.). Above 1250 °C, the relative density falls off towards a minimum value of 60.8% at 1350 °C. This may be attributed to the swelling of samples and formation of large pores as confirmed by SEM investigation (Fig. 3). Indeed, the cordierite formed at 1300 °C showed a porous structure with pores size between 10 and 120 µm. A particularly low density was observed at 1350 °C; the pores are perfectly spherical with size between 10 and 400 µm in diameter.

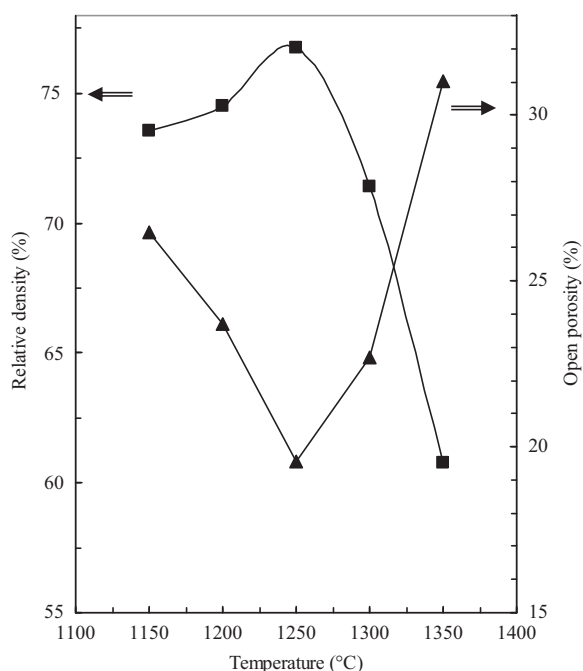


Fig. 2. Open porosity and relative density evolution of sintered samples.

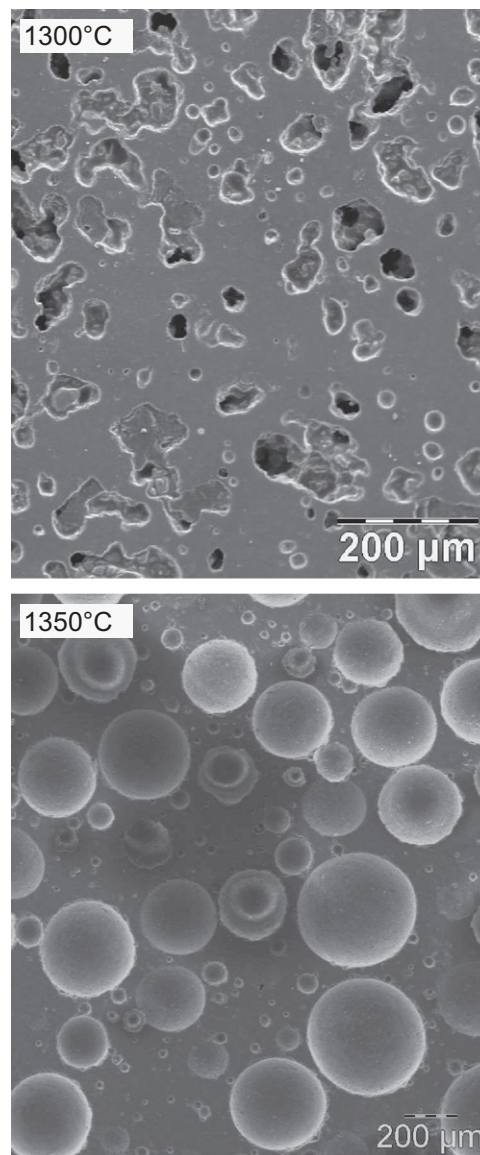


Fig. 3. SEM micrographs of cordierite sintered at 1300 and 1350 °C.

### 3.3. Mechanical properties

Three-point bending test, Brazilian test and ultrasonic testing were used to study the evolution of mechanical behavior and to evaluate the elastic properties of samples sintered between 1150 and 1350 °C. For each temperature, three similar specimens were prepared in order to verify the reproducibility of the test results.

#### 3.3.1. Three-point bending test

Fig. 4 shows typical load–deflection curves of samples sintered at 1200 °C, 1250 °C and 1300 °C. As shown, samples exhibit a linear-elastic behavior up to brittle failure. Several discontinuities were observed on the loading curves for samples sintered at 1200 and 1250 °C. This may be explained by the high porosity and hence the progressive crushing of insufficiently densified samples.

The amorphous phase, created during sintering at 1200 and 1250 °C is insufficient to form bridges between the grains. When sufficient vitreous phase is formed at 1300 °C, this serrated trend transforms into a smooth behavior.

The flexural strength increases significantly from  $23.46 \pm 1.8$  to  $43.31 \pm 1$  MPa as the firing temperature increases from 1200 to 1250 °C. This strength enhancement can be attributed to the increase in density when the sintering temperature is raised (Table 1). However, a relative decrease in flexural strength is observed to reach  $39.73 \pm 4$  MPa for cordierite synthesized at 1300 °C. This result may be due to the swelling of sample and the formation of large pores, as shown in Fig. 3. As predicted by several models, the mechanical properties decrease with increasing porosity. For example, the following mathematical model shows that the flexural strength decreases exponentially with increasing porosity [21]:

$$\sigma(P) = \sigma_0 \exp(-bP) \quad (12)$$

where  $\sigma_0$  is the strength of pore-free materials,  $b$  is an empirical constant and  $P$  is the volume fraction of pores.

For comparison, the flexural strength of cordierite synthesized in this study at 1300 °C is much lower than values

obtained in previous works for dense cordierite (70–110 MPa) [22,23], but it is similar or higher than those reported for porous cordierite [24–26].

### 3.3.2. Brazilian test

Fig. 5 shows a typical load–displacement curve for the diametral compression test on samples sintered at 1200 °C and 1300 °C. These results confirm the linear elastic and brittle behavior observed in the three-point bending test. In the first step, the load increases gradually with an important deformation. This behavior was also explained by the appearance of multiple discontinuities observed in the three-point bending test. In the second step, the behavior is perfectly linear elastic up to brittle fracture. A relative decrease in tensile strength is observed when increasing temperature from 1200 °C to 1300 °C. The tensile strength values of samples sintered at 1200 °C and 1300 °C are 23.1 and 21.8 MPa, respectively. The tensile strength of cordierite obtained in this study at 1300 °C is relatively lower than that of industrial batch (25.5 MPa) [27].

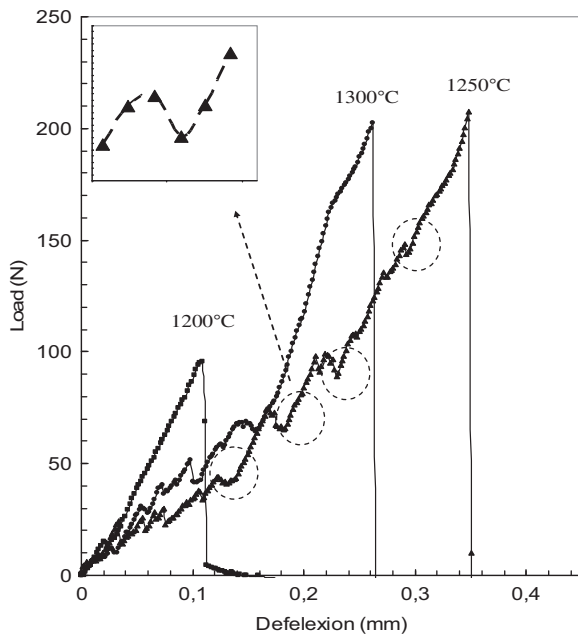


Fig. 4. Flexural load–displacement curves of sintered samples.

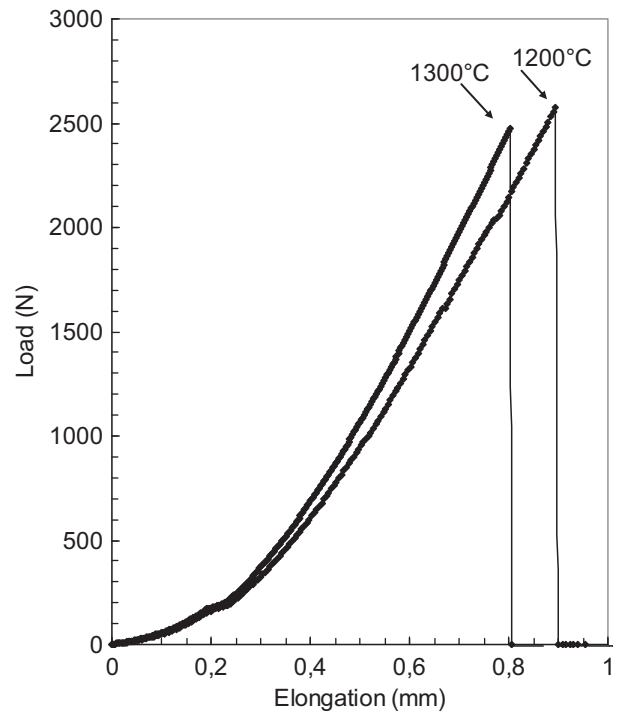


Fig. 5. Typical load–displacement curves of samples under diametral compression.

Table 1  
Effect of sintering temperature on densification and flexural strength.

Sintering temperature (°C)	Relative density (%)	Open porosity (%)	Flexural strength (MPa)	Deflection at failure (mm)
1200	74.5	23.7	$23.46 \pm 1.8$	0.11–0.19
1250	76.8	19.6	$43.31 \pm 1$	0.35–0.42
1300	71.4	22.7	$39.73 \pm 4$	0.23–0.26



### 3.3.3. Elastic properties

The evolution of dynamic elastic properties determined by ultrasonic non-destructive testing of cordierite synthesized at 1300 and 1350 °C is summarized in Table 2. These results show that Young's modulus decreases from 45.2 to 38.7 GPa when the sintering temperature increases from 1300 to 1350 °C. This can be attributed to the higher porosity observed at 1350 °C (Fig. 3). Indeed, an increase of the porosity from 22.7% at 1300 °C to 31.2% at 1350 °C was observed (Fig. 2). Dean et al. [21] observed a linear decrease of the Young's modulus with the increase in porosity according to the linear relationship:

$$E(P) = E_0 (1 - \varepsilon P) \quad (13)$$

where  $E_0$  is Young's modulus of pore-free material,  $\varepsilon$  is an empirical constant and  $P$  is the volume fraction of pores.

Young's modulus values were relatively low compared to dense cordierite, namely by Rohan et al. [28] ( $55 \pm 3$  GPa for a density of  $2.54 \text{ g cm}^{-3}$ ), (70 GPa for a density of  $2.6 \text{ g cm}^{-3}$ ) [27]. However, the  $E$  values were higher than those reported for porous cordierite, namely by Ozel and Kurama [15] (37 GPa for a density of  $2.45 \text{ g cm}^{-3}$ ), Costa-Oliveira et al. [16] (1–5 GPa for a density of  $0.37\text{--}0.59 \text{ g cm}^{-3}$ ), Dimitrijevic et al. [29] (0.87 GPa for a density of  $1.75 \text{ g cm}^{-3}$ ).

Similar to Young's modulus, Poisson's ratio ( $\nu$ ) values of cordierite decreases from 0.16 to 0.08, when the temperature increased from 1300 to 1350 °C, as result of increase in porosity. The  $\nu$  values were very small compared to that of dense cordierite (0.21) [27]. Comparison between static Young's modulus ( $E_S$ ) and dynamic Young's modulus ( $E_D$ ) of cordierite synthesized at 1300 °C shows an important discrepancy. The  $E_S$  value estimated from Eq. 2 using flexural test and the  $E_D$  value from Eq.5 by ultrasonic tests were  $11.5 \pm 0.9$  and  $45.2 \pm 3$  GPa, respectively. The ratio of dynamic to static modulus was approximately 4.

## 4. Conclusion

The following conclusions can be drawn from the present investigation on the microstructural and mechanical characterization of cordierite-based ceramics produced from stevensite–andalusite mixture:

- (1) The optimum sintering temperatures for the synthesis of cordierite as a main phase, with traces of mullite, are 1300 and 1350 °C.
- (2) The density measurements and SEM observations indicated that cordierite produced at 1350 °C is highly porous compared to that formed at 1300 °C.
- (3) The flexural strengths ( $39.4 \pm 4$  MPa) and tensile strengths ( $21.8 \pm 2$  MPa) values of cordierite produced at 1300 °C are relatively lower and this result can be attributed to the increase in porosity.
- (4) A linear brittle elastic behavior was observed with the presence of multiple discontinuities during loading in the three-point bending test.
- (5) The results of Young's modulus measurements on the samples fired at 1300 and 1350 °C show that the increase in porosity with sintering temperature is the most important cause of the decrease of the values of Young's modulus from 45.2 to 38.7 GPa.

## References

- [1] O. Owate, R. Freer, The electrical properties of some cordierite glass ceramics in the system  $\text{MgO-Al}_2\text{O}_3\text{-SiO}_2\text{-TiO}_2$ , *Journal of Materials Science* 25 (1990) 5291–5297.
- [2] D.D. Stoyanova, D. Ch. Vladov, N.A. Kasabova, D.R. Mekhandzhiev, Cordierite-like catalyst supports based on clay materials, *Kinetics and Catalysis* 46 (2005) 609–612.
- [3] G.H. Beall, Refractory glass–ceramics based on alkaline earth aluminosilicates, *Journal of the European Ceramic Society* 29 (2009) 1211–1219.
- [4] D.N. Boccacini, C. Leonelli, M.R. Rivasi, M. Romagnoli, A.R. Boccacini, Microstructural investigations in cordierite–mullite refractories, *Ceramics International* 31 (2005) 417–432.
- [5] E. Sun, Y.H. Choa, T. Sekino, K. Niihara, Fabrication and mechanical properties of cordierite/ $\text{ZrO}_2$  composites by pressureless sintering, *Journal of Ceramic Processing Research* 1 (2000) 9–11.
- [6] Y.J. Oh, T.S. Oh, H.J. Yung, Microstructure and mechanical properties of cordierite ceramics toughened by monoclinic  $\text{ZrO}_2$ , *Journal of Materials Science* 26 (1991) 6491–6649.
- [7] D. Manfredi, M. Pavese, S. Biamino, A. Antonini, P. Fino, C. Badini, Microstructure and mechanical properties of co-continuous metal/ceramic composites obtained from reactive metal penetration of commercial aluminium alloys into cordierite, *Composites: Part A* 41 (2010) 639–645.
- [8] R. Goren, H. Gocmez, C. Ozgur, Synthesis of cordierite powder from talc, diatomite and alumina, *Ceramics International* 32 (2006) 407–409.
- [9] K. Zhu, D.Y. Yang, J. Wu, R. Zhang, Synthesis of Cordierite with Low Thermal Expansion Coefficient, *Advanced Materials Research* 105 (2010) 802–804.
- [10] Z. Acimovic, L. Pavlovic, L. Trumbulovic, L. Andric, M. Stamatovic, Synthesis and characterization of the cordierite ceramics from non-standard raw materials for application in foundry, *Materials Letters* 57 (2003) 2651–2656.
- [11] S. Kumar, K.K. Singh, P. Ramachandrarao, Synthesis of cordierite from fly ash and its refractory properties, *Journal of Materials Science Letters* 19 (2000) 1263–1265.
- [12] J.C. Bernier, J.L. Rehspringer, S. Vilminot, P. Poix, Synthesis and sintering comparison of cordierite powders, *Materials Research Society, Proceedings* 73 (1986) 129–134.
- [13] N.T. Andrianov, S.R. Abdel-gavad, N.V. Zenkova, Synthesis and sintering of cordierite sol–gel powders based on different magnesium salts, *Glass and Ceramics* 63 (2006) 415–418.

Table 2  
Effect of sintering temperature on elastic properties.

	1300 °C	1350 °C
Apparent density ( $\text{g cm}^{-3}$ )	1.91	1.61
Longitudinal velocity ( $\text{m s}^{-1}$ )	5046	4935
Transversal velocity ( $\text{m s}^{-1}$ )	3203	3333
Young modulus $E_D$ (GPa)	45.15	38.68
Shear modulus $G$ (GPa)	19.42	17.90
Poisson ratio $\nu$	0.16	0.08

- [14] E.M.M. Ewais, Y.M.Z. Ahmed, A.M.M. Ameen, Preparation of porous cordierite ceramic using a silica secondary resource (silica fumes) for dust filtration purposes, *Journal of Ceramic Processing Research* 1 (2009) 721–728.
- [15] E. Ozel, S. Kurama, Effect of the processing on the production of cordierite-mullite composite, *Ceramics International* 36 (2010) 1033–1039.
- [16] F.A. Costa Oliveira, J. Cruz Fernandes, Mechanical and thermal behaviour of cordierite–zirconia composites, *Ceramics International* 28 (2002) 79–91.
- [17] A. Benhammou, B. Tanouti, L. Nibou, A. Yaacoubi, J.P. Bonnet, Mineralogical and physicochemical investigation of Mg–smectite from Jbel Ghassoul, Morocco, *Clays and Clay Minerals* 57 (2009) 264–270.
- [18] A. Arib, R. El Quatib, T. Remmal, R. Moussa, Thermal behaviour and structural transformations of andalusite-rich aluminous nodules from Morocco, *Key Engineering Materials* 264 (2004) 1815–1818.
- [19] S. Shimoda, Mineralogical studies of a species of stevensite from the Obori Mine, Yamagata Prefecture, *Japanese Clay Minerals* 9 (1971) 85–192.
- [20] W. Pannhorts, H. Schneider, The high-temperature transformation of andalusite ( $\text{Al}_2\text{SiO}_5$ ) into 3/2 mullite ( $3\text{Al}_2\text{O}_3\text{--}2\text{SiO}_2$ ) and vitreous silica ( $\text{SiO}_2$ ), *Mineralogical Magazine* 42 (1978) 195–198.
- [21] E.A. Dean, J.A. Lopez, Empirical dependence of elastic moduli on porosity for ceramic materials, *Journal of the American Ceramic Society* 66 (1983) 366–370.
- [22] S.J. Lee, W.M. Kriven, Fabrication of low thermal expansion and low dielectric ceramic substrates by control of microstructure, *Journal of Ceramamic Processing Research* 4 (2003) 118–121.
- [23] H. Shao, K. Liang, F. Peng, F. Zhou, A. Hu, Production and properties of cordierite-based glass–ceramics from gold tailings, *Minerals Engineering* 18 (2005) 635–637.
- [24] S. Liu, Y.P. Zeng, D. Jiang, Effects of  $\text{CeO}_2$  addition on the properties of cordierite-bonded porous SiC ceramics, *Journal of European Ceramic Society* 29 (2009) 1795–1802.
- [25] S. Zhu, S. Ding, H. Xi, Q. Li, R. Wang, Preparation and characterization of SiC/cordierite composite porous ceramics, *Ceramic International* 33 (2007) 115–118.
- [26] Y. He, W.M. Cheng, H. Cai, Characterization of cordierite glass–ceramics from fly ash, *Journal of Harzardous Materials B120* (2005) 265–269.
- [27] Online: <[http://www.ferroceramic.com/Cordierite\\_table.htm](http://www.ferroceramic.com/Cordierite_table.htm)>, (2010).
- [28] P. Rohan, K. Neufuss, J. Matejíček, J. Dubský, L. Prchlík, C. Holzgartner, Thermal and mechanical properties of cordierite, mullite and steatite produced by plasma spraying, *Ceramics International* 30 (2004) 597–603.
- [29] M. Dimitrijevic, M. Posarac, J. Majstorovic, T. Volkov-Husovic, B. Matovic, Behavior of silicon carbide/cordierite composite material after cyclic thermal shock, *Ceramics International* 35 (2009) 1077–1081.